D^*-PRODUCTION AND F_2^c FOR $Q^2 > 1\,\mathrm{GEV}^2$

S. MOHRDIECK

for the H1 Collaboration

II. Institut f. Experimentalphysik, Universität Hamburg, Luruper Chaussee 149, 22761 Hamburg, Germany

Results of the H1 experiment on the visible ep cross section for inclusive $D^*(2010)$ meson production in deep-inelastic scattering are presented in a kinematic range of $1 < Q^2 < 100\,\mathrm{GeV}^2$ and $0.05 < y < 0.7$ and in the visible region $p_t(D^*) > 1.5\,\mathrm{GeV}$ and $|\eta(D^*)| < 1.5$. The data is compared to predictions based on perturbative QCD calculations in the CCFM and NLO DGLAP scheme. The charm contribution to the proton structure function, F_2^c, is extracted by extrapolating the visible cross section to the full phase space.

1 Charm Production, Theoretical Models and Selection

Charm production in ep collisions is dominated by photon gluon fusion ($\gamma g \rightarrow c\bar{c}$). The process of charm production can be calculated in the framework of perturbative QCD. Calculations for various schemes and different evolutions of the QCD dynamics are available.

In the analysis presented[1] the charm quark is identified by the reconstruction of a D^* meson in its decay via a D^0 meson into $\mathrm{K}\pi\pi$. Important kinematic variables are the virtuality of the photon Q^2, the Bjorken variables x and y, the transverse momentum p_t of the D^* meson and its pseudo rapidity η.

Here the experimental results are compared to predictions using the HVQDIS[2] program, which is based on the NLO DGLAP evolution and uses the Peterson fragmentation function[3] for fragmenting charm quarks into D^* mesons. The fragmentation is controlled by a single parameter, ϵ_c. The data is also compared to predictions based on the CCFM[4] evolution as implemented in the Monte Carlo event generator CASCADE[5].

The data presented here were recorded with the H1 detector in the years 1996 and 1997 and correspond to an integrated luminosity of $18.6\,\mathrm{pb}^{-1}$. The decay particles of the D^* meson are reconstructed in the central region of the detector. The data is restricted to the range $p_t(D^*) > 1.5\,\mathrm{GeV}$ and $|\eta(D^*)| < 1.5$. A scattered electron is detected in the backward calorimeter of H1. The results cover a kinematic region of $1 < Q^2 < 100\,\mathrm{GeV}^2$ and $0.05 < y < 0.7$ where 973 ± 40 D^* mesons are observed.

2 Results on inclusive D^*-Production

The visible cross section of inclusive D^* production is measured to be $\sigma(ep \to eD^*X) = (8.50 \pm 0.42(stat.)^{+1.21}_{-1.00}(syst.))$ nb. This result is compared to the predictions of HVQDIS (NLO DGLAP) and CASCADE (CCFM) which yield visible cross sections of 5.17 to 7.02 nb and 8.04 to 10.77 nb respectively. The lower values are for $m_c = 1.5$ GeV and $\epsilon_c = 0.1$ while the upper limits correspond to $m_c = 1.3$ GeV and $\epsilon_c = 0.035$. The expectation of CASCADE is in better agreement with the data than the prediction of HVQDIS.
Single differential cross sections in the kinematic variables x and Q^2 as well as in the pseudo rapidity η_{D^*} of the D^* meson are shown in fig.1a). The results are compared to predictions of HVQDIS and CASCADE as indicated by the shaded error bands. The width of the band is given by varying ϵ_c and m_c. Although HVQDIS falls somewhat below the data in normalization, the

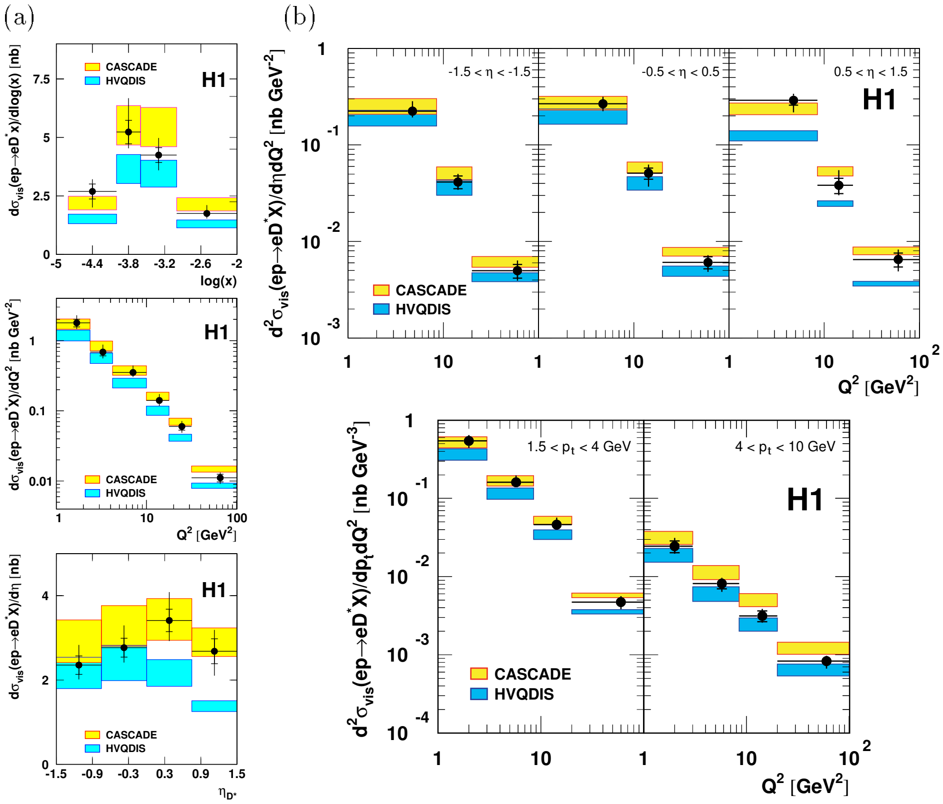

Figure 1. Single (a) and double (b) differential visible cross sections for inclusive D^* production.

behaviour of the data is well described in most cases. Only at large pseudo rapidity $\eta(D^*)$ discrepancies are seen. Here the data exceeds the theoretical prediction. The excess is found to be independent of Q^2 and is located in the region of small $p_t(D^*)$, as it is shown in fig.1b) by analysing double differential cross sections. In general CASCADE provides a better description of the data, both in normalization and shapes.

3 Results on F_2^c

The charm contribution to the proton structure function, F_2^c, is extracted by extrapolating the visible cross section to the full phase space using predictions from theoretical models according to:

$$F_2^c(x, Q^2) = \sigma_{vis}^{meas}(x, Q^2) \cdot \frac{F_2^{c\,theo}(x, Q^2)}{\sigma_{vis}^{theo}(x, Q^2)}, \qquad (1)$$

where $F_2^{c\,theo}$ and σ_{vis}^{theo} are the theoretical predictions of the model under consideration, σ_{vis}^{meas} is the measured cross section in the visible region. Fig.2a) shows F_2^c as a function of x for different values of Q^2 extracted in the NLO DGLAP scheme[2,6]. The measurement is compared to the theoretical prediction of F_2^c using the gluon distributions from the H1 NLO DGLAP fit[7] to the inclusive F_2 data. The error band indicates the total uncertainty of the

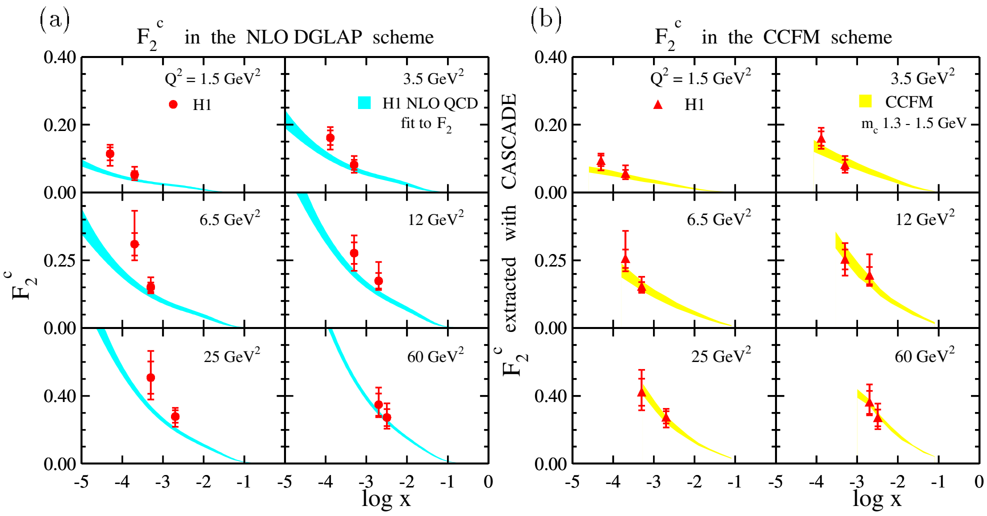

Figure 2. F_2^c as function of x for different values of Q^2. In (a) F_2^c is extracted in the NLO DGLAP scheme, in (b) F_2^c is extracted in the CCFM scheme.

prediction resulting from the uncertainties on this fit. It is dominated by the error due to the charm quark mass. An F_2^c extraction based on CCFM yields a different structure function since the corrections to the full phase space are different. The result is shown in fig.2b). F_2^c extracted in the NLO DGLAP scheme lies systematically above F_2^c from CCFM. The discrepancy becomes as large as 20% at small x.

4 Conclusions

Results on inclusive D^* production cross sections in deep-inelastic scattering have been presented. Single and double differential distributions have been compared to predictions of HVQDIS (NLO DGLAP scheme) and the CCFM based Monte Carlo event generator CASCADE. The predictions of CASCADE are in better agreement with the data than HVQDIS, where differences at large η_{D^*} and small p_{t,D^*} are seen.
Results for the measurement of F_2^c have been derived for the two different schemes (NLO DGLAP and CCFM) which differ because of different extrapolations.

References

1. C. Adloff et al. (H1 Collaboration), "Measurement of $D^{*\pm}$ Meson Production and F_2^c in Deep-Inelastic Scattering at HERA", DESY-01-100, to be submitted to Phys. Lett. B
2. B.W. Harris and J. Smith, Nucl. Phys. B452 (1995) 109, Phys. Lett. B353 (1995) 535; B.W. Harris and J. Smith, Phys. Rev. D57 (1998) 2806.
3. C. Peterson et al., Phys. Rev. D27 (1983) 105.
4. M. Ciafaloni, Nucl. Phys. B296 (1988) 49; S. Catani, F. Fiorani and G. Marchesini, Phys. Lett. B234 (1990) 339; Nucl. Phys. B336 (1990) 18; G. Marchesini, Nucl. Phys. B445 (1995) 49.
5. H. Jung, Proc. 7th DIS Workshop, Nucl. Phys. B (Proc. Suppl.) 79 (1999) 429; H. Jung, Proc. Workshop on Monte Carlo Generators for HERA Physics, 1998-1999, DESY-PROC-1999-02, p.75; H. Jung and G. Salam, hep-ph/0012143, Euro. Phys. J. C19 (2001) 351.
6. E. Laenen et al., Phys. Lett. B291 (1992) 325; E. Laenen et al., Nucl. Phys. B392 (1993) 162, 229; S. Riemersma, J. Smith, and W.L. van Neerven: Phys. Lett. B347 (1995) 143.
7. C. Adloff et al. (H1 Collaboration), DESY-00-181, hep-ex/0012053, submitted to Eur. Phys. J. C.